PHYSICAL REVIEW B **79**, 172407 (2009)

Ab initio study of hyperfine interaction parameters in *C*14 Hf and Zr Laves-phase compounds

Jelena Belošević-Čavor, V. Koteski, J. Radaković, and B. Cekić
Institute of Nuclear Sciences Vinča, P.O. Box 522, 11001 Belgrade, Serbia

(Received 25 November 2008; revised manuscript received 7 April 2009; published 18 May 2009)

Using *ab initio* density-functional theory approach the electric field gradients (EFGs) and hyperfine magnetic fields (HMFs) for the isostructural *C*14 Laves-phase compounds $\mathrm{HfCr_2}$, $\mathrm{HfFe_2}$, $\mathrm{HfMn_2}$, $\mathrm{ZrCr_2}$, and $\mathrm{ZrMn_2}$ are calculated and compared with the available experimental data from time differential perturbed angular-correlation (TDPAC) spectroscopy. In addition, supercell calculations of the hyperfine interaction parameters at the nucleus of the substitutional Ta impurity are used to elucidate the role played by the Ta probe in the TDPAC measurements of Hf and Zr *C*14 Laves phases and solve the controversy related to the origin of the HMF in the *C*14 $\mathrm{HfFe_2}$ compound.

DOI: 10.1103/PhysRevB.79.172407 PACS number(s): 71.20.Be, 71.15.Ap, 75.50.Cc

3*d* Laves-phase intermetallic compounds show a number of interesting features including polymorphism and peculiar magnetic properties.[1–3] These compounds are also considered as hydrogen storage materials.[4–7] The nonmagnetic Cr-based Laves-phase compounds $\mathrm{ZrCr_2}$ and $\mathrm{HfCr_2}$ are of technological interest because of potential applications as high-temperature structural materials with excellent corrosion and oxidation resistance.[8] The structural and phase stabilities, as well as enthalpies of formation for these compounds, have been calculated by employing ultrasoft pseudopotentials within the generalized gradient approximation (GGA).[9,10] Mn-based Laves phases, $\mathrm{HfMn_2}$ and $\mathrm{ZrMn_2}$, are of interest because of their, known or predicted, magnetic properties.[2,3,11] Based on the results of a Korringa-Kohn-Rostoker approach, Ishida *et al.*[12] concluded that in the *C*14 $\mathrm{ZrMn_2}$ structure, Mn atoms at the 2*a* lattice sites might carry a magnetic moment and be ferromagnetically ordered. From linear muffin-tin orbital (LMTO) calculations, Asano and Ishida[13,14] drew the same conclusion, but they also pointed out that according to their results for the *C*14 $\mathrm{ZrMn_2}$ structure the ferromagnetic and nonspin-polarized states are degenerate in energy. Very recently, Chen *et al.*[2,3] concluded that for *C*14 $\mathrm{HfMn_2}$ and $\mathrm{ZrMn_2}$, there is a strong indication of magnetic ordering, but this has not been verified experimentally.[11]

Our purpose in this work is to investigate the EFGs and HMFs in the 3*d* Laves-phase Hf and Zr intermetallic compounds and thus obtain information about the symmetry of charge distribution around the nucleus. The existence of nonzero-hyperfine magnetic fields is also an indication that some kind of strong magnetic ordering is present in the investigated solid. In addition, we want to elucidate a controversy which has been present in the literature for a long time. Namely, due to the similarity of the *C*14 and *C*15 Laves-phase crystal structures, it has been virtually impossible to determine with certainty the TDPAC measured value of the HMF in the *C*14 $\mathrm{HfFe_2}$ system, and the reported results differ from each other substantially.[15–17] Recently reported calculations[18] for pure *C*14 $\mathrm{HfFe_2}$ compound failed to shed new light on this discrepancy, as the obtained value markedly differs from all the reported experimental values, which is most likely a consequence of the neglect of the impurity effect. Using a supercell calculation approach with Ta substituting at Hf lattice site, we are able to undoubtedly identify the correct value for the HMF in this compound.

*C*14 is $\mathrm{MgZn_2}$-type structure (space-group $P6_3/mmc$). It possesses three nonequivalent crystallographic positions (4*d*, 2*a*, and 6*h*) and two internal parameters, u and v, which determine position of Mg (in our case Hf) (1/3, 2/3, and u) and Zn (in our case Cr, Fe, and Mn) (v, $2v$-1, and 0.25).

The calculations have been performed using the augmented plane wave plus local orbitals (APW+lo) method as implemented in the WIEN2K code,[31] within the framework of the DFT.[32] All reported results are obtained from fully relaxed structures with respect both to the cell parameters and internal degrees of freedom. The calculations were carried out with 76 k points in the irreducible wedge of Brillouin zone (IBZ) and plane-wave cutoff parameter $R_{\mathrm{mt}}K_{\mathrm{max}}=7.0$. We also did a test case with $R_{\mathrm{mt}}K_{\mathrm{max}}=8.0$ and 135 k points in the IBZ and found that the differences in the calculated EFGs and HMFs were 1.5–2.5 %, so for the further calculations we adopted the above mentioned values. Muffin-tin (MT) radii for Hf and Ta were 2.3, for Zr, Fe, and Mn 2.2, and for Cr 2.1 a.u. The exchange-correlation potential was calculated by the GGA with the parametrization given by Ref. 33. The threshold energy between valence and core states was −7 Ry in order to include low-laying *s* states of 3*d* elements. The core states were treated fully relativistically, while the valence states were treated within the scalar relativistic approximation. Because of the large atomic numbers of Ta and Hf, spin-orbit coupling for these atoms was included in the calculations. In our calculations the self-consistency was achieved by demanding the convergence of the integrated charge difference between last two iterations to be smaller than 10^{-5} electron.

The calculated cell and structure parameters for the investigated compounds, along with the values obtained from x-ray diffraction measurements and earlier calculations are presented in Table I. In most of the cases the theoretical volume underestimates the experimental one, but the overall agreement with the previously reported values is good. The bulk moduli B_0 obtained by fitting the data to the Murnaghan's equation of state[34] are also given in Table I and they agree well with some of the earlier reported calculated data.

After determining the self-consistent charge density we obtained the EFG tensor V_{ij} using the method developed in Ref. 35. The usual convention is to designate the largest component of the EFG tensor as V_{zz}. The asymmetry parameter η is then given by $\eta=(V_{yy}-V_{xx})/V_{zz}$, where $|V_{zz}|$

©2009 The American Physical Society

TABLE I. Structure parameters of the investigated $C14$ compounds. Experimental values are taken from Refs. 2, 3, 9, 11, and 18–30. The distances are in Å.

	Experimental results (x-ray diffraction)	WIEN2K	Earlier calculations
	$HfCr_2$		
a	5.067^a	5.032	5.046^a
c	8.237^a	8.116	8.095^a
u		0.0608	
B		204	191^a, 173^b
	$HfMn_2$		
a	4.990,[c] 4.956,[d] 5.000^e	4.858	4.915^f
c	8.21,[c] 8.122,[d] 8.205^e	8.147	8.149^f
u		0.0637	
v		0.8295	
B		190	194^f
	$HfFe_2$		
a	$4.974(1)^g$	4.941	4.946^g
c	$8.114(3)^g$	8.01	8.032^g
u	0.065^g	0.063	0.062^g
v	0.824^g	0.8318	0.832^g
B		154	166^g
	$ZrCr_2$		
a	5.089,[h] $5.103(2)^i$	5.076	5.094^a
c	8.28,[h] $8.268(4)^i$	8.123	8.103
u	$0.0603(3)^i$	0.06025	
v	$0.8317(9)^i$	0.8325	
B		163	155,[b] 176,[a] 181,[h] 187^h
	$ZrMn_2$		
a	5.029,[j] $5.033(1)$,[k] 5.016,[l] 5.026,[n] 5.041,[n] 5.046,[p] 5.030^q	4.895	4.937^m
c	8.266,[j] $8.275(3)$,[k] 8.255,[l] 8.258,[n] 8.249,[n] 8.295,[p] 8.264^q	8.280	8.242^m
u		0.0642	0.4364^m
v		0.8302	0.8304^m
B		164	204,[h] 209,[h] 180,[m] 149^j

[a] Reference 9.
[b] Reference 30.
[c] Reference 27.
[d] Reference 26.
[e] Reference 28.
[f] Reference 3.
[g] Reference 18.
[h] Reference 21.
[i] Reference 20.
[j] Reference 11.
[k] Reference 19.
[l] Reference 29.
[m] Reference 2.
[n] Reference 22.
[o] Reference 23.
[p] Reference 24.
[q] Reference 25.

$\geq |V_{yy}| \geq |V_{xx}|$. Our calculated EFG can be represented as a sum of two terms: the valence one (V_{zz}^{val}), originating from the nonspherical charge within MT spheres and the lattice one (EFG-V_{zz}^{val}), which stems from the interstitial charge and is usually only a small correction. In Table II, the decomposition of the EFGs at all three non-equivalent lattice sites in the fully relaxed structures of the investigated compounds are presented. We also predict the signs of the EFGs, which have not been determined experimentally. The EFGs at the two transition-metal (TM) sites ($2a$ and $6h$) have opposite signs when compared with the EFGs at Hf(Zr), except for the Mn compounds. As it is often the case in the TM compounds, the main contribution to the EFG at all three sites in all the investigated compounds comes from the p electrons. The contribution from the d electrons is generally much smaller and is comparable with the p contribution only at Cr $2a$ site in $HfCr_2$ and at Mn $6h$ site in both Mn compounds. The calculated EFGs in the Hf compounds are significantly larger than the corresponding ones in the Zr compounds, as is also the case in many other isostructural Hf and Zr intermetallics.[36,37] If we compare the onsite contribution to the EFG (V_{zz}^{val} in Table II) with the lattice contribution (EFG-V_{zz}^{val}), it is clear that the latter is virtually zero at the Hf(Zr) site and has small values at TM $2a$ and $6h$ sites.

The calculated spin-magnetic moments (MMs) obtained as a difference of the number of electrons with spin up and down inside the muffin-tin spheres, are shown in Table III. The main contribution to the MMs comes from the spin polarization of the d states. As a general feature, the calculated MMs of Hf and Zr have an opposite direction from that of the TM atoms. The relatively small magnitude of the MMs of Hf and Zr implies that they are generated by the atomic crystal environment. Comparing the MMs that correspond to the three crystallographic positions in the $C14$ structure, we can see that they are decreasing as we go from $HfFe_2$ via $ZrMn_2$ to $HfMn_2$. Interestingly, the magnitude of the MM of the Fe atoms at the two different lattice sites is very similar in $HfFe_2$, whereas in $HfMn_2$ and $ZrMn_2$ the magnetic moment of atom at $2a$ is twice as large as the one at $6h$ positions. All calculated MMs agree well with the previously reported values given in Table III. The main contribution to the calculated HMFs presented in Table III is the Fermi contact interaction, calculated according to Ref. 39. The largest HFM is found in $HfFe_2$, in agreement with the largest magnetic-moment values in this compound. The calculated values for this compound are similar as those reported in reference 18, which is expected because of the similarity of methods used full-potential linearized augmented-planewave

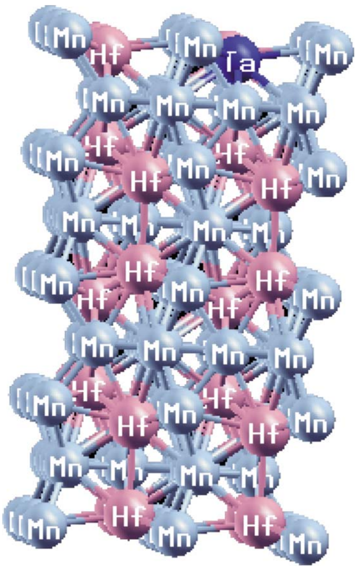

FIG. 1. (Color online) 96-atom supercell in 2×2×2 geometry of $HfMn_2$:Ta, produced by XCRYSDEN visualization code (Ref. 38).

TABLE II. Decomposition of the calculated V_{zz}^{val} values in units of 10^{21} V/m^2 for the fully relaxed structures of the investigated compounds.

	p-p	d-d	Others	V_{zz}^{val}	EFG	η
$HfCr_2$						
Cr 2a	−0.8584	−0.6204	−0.0376	−1.516	−1.42	0
Cr 6h	−1.1112	0.1536	−0.0341	−1.2009	−1.12	0.585
Hf 4f	3.384	0.2695	0.0035	3.657	3.66	0
$HfMn_2$						
Mn 2a	−3.9764	1.3132	−0.0263	−2.6895	−2.64	0
Mn 6h	−2.868	2.0154	−0.0514	−0.904	−0.81	0.056
Hf 4f	−1.3458	0.6875	0.0277	−0.6306	−0.64	0
$HfFe_2$						
Fe 2a	−3.7337	0.9143	−0.0368	−2.8562	−2.789	0
Fe 6h	−3.5634	0.9071	−0.0311	−2.6874	−2.64	0.26
Hf 4f	0.2195	0.0329	−0.0432	0.2092	0.215	0
$ZrCr_2$						
Cr 2a	−1.2223	−0.264	−0.0411	−1.5275	−1.43	0
Cr 6h	−1.7842	−0.4169	−0.0329	−1.4267	−1.36	0.629
Zr 4f	2.3065	0.1196	−0.0064	2.4197	2.44	0
$ZrMn_2$						
Mn 2a	−4.3536	1.8406	−0.0226	−2.5356	−2.509	0
Mn 6h	−3.0806	2.1277	−0.0484	−1.0009	−0.9184	0.505
Zr 4f	−0.7195	0.4575	0.0043	−0.2577	−0.2604	0

(FP-LAPW). HMFs at 2a and 6h positions in all the investigated compounds have similar values, but the one at Hf(Zr) lattice site is considerably larger. The HMFs can be decomposed to core B_c and valence contributions B_v. For Hf(Zr), B_v is dominant, originating from the spin polarization of the valence electrons due to the magnetic moment at the TM atoms. For the TM atoms, B_c is dominant although B_v is significant too. The existence of nonzero HMFs in the $HfMn_2$ and $ZrMn_2$ compounds should be considered as a strong argument which supports the claim of strong magnetic ordering at 0 K.[2,3]

Hyperfine interaction measurements exist only for the two

TABLE III. Calculated magnetic moments (μ_B) and hyperfine magnetic fields (B_{hf}) in $HfFe_2$, $ZrMn_2$, and $HfMn_2$. The μ_B is decomposed to various atomic contributions. The decomposition of B_{hf} into valence (B_V), and core (B_c) contribution is also given. The experimental values are taken from Refs. 1, 7, 10, and 18.

Atom	s	p	d	f	WIEN2K μ_B	Earlier calculations μ_B	B_V [T]	B_c [T]	B_{hf} [T]
$HfFe_2$									
Hf	−0.0097	−0.0294	−0.235	0.0014	−0.273	0.264[a]	−31.24	−0.82	−32.06
Fe 2a	0.0043	−0.0310	1.8761	0.0009	1.850	1.84[a]	31.76	−48.76	−17.00
Fe 6h	0.0030	−0.0203	1.8704	0.0005	1.854	1.853[a]	30.03	−48.62	−18.59
$HfMn_2$									
Hf	−0.0055	−0.0097	−0.0702	0.0016	−0.084		−21.84	−0.33	−22.16
Mn 2a	0.0057	−0.0004	1.0670	0.0005	1.073	1.1[b]	18.29	−24.35	−6.06
Mn 6h	0.0006	−0.0073	0.5152	0.0007	0.509	0.5[b]	6.46	−11.95	−5.49
$ZrMn_2$									
Zr	−0.0048	−0.0093	−0.092	0.0007	−0.105		−13.70	0.17	−13.53
Mn 2a	0.0077	0.0001	1.2512	0.0005	1.259	1.24,[c]1.03[d]	21.10	−27.84	−6.73
Mn 6h	0.0008	−0.0079	0.5489	0.0007	0.542	0.60,[c]0.62[d]	6.37	−12.39	−6.02

[a] Reference 18.

[b] Reference 10.

[c] Reference 1.

[d] Reference 7.

TABLE IV. Comparison between the calculated and measured EFG and HMF values at ^{181}Ta position in the investigated compounds. The measured values refer to room temperature.

	EFG $[10^{21}\ \mathrm{V/m^2}]$		B_{hf} $[T]$	
Phase	Measured	Calculated	Measured	Calculated
$HfCr_2$		2.17		
$HfFe_2$	±0.37 [ab]	−0.73	±8.2(3) [b]	−11.0
$HfMn_2$		−2.42		−0.08
$ZrCr_2$	±1.02 [c]	1.26		
$ZrMn_2$		0.55		−27.5

[a] Measured at 453 K.
[b] Reference 17.
[c] Reference 20.

of these five compounds, $ZrCr_2$ (Ref. 14) and $HfFe_2$,[15–17] and they have been done by employing the TDPAC method in which the measurement actually takes place on the ^{181}Ta probe ion instead on the Hf nucleus. Because of that fact, it was necessary to perform supercell calculations (Fig. 1).The results obtained in such a way are given in Table IV.

For $ZrCr_2$ the agreement between the measured and the calculated EFG is very good, especially considering its small absolute value. In the case of the $C14$ $HfFe_2$ the situation is more complicated, as the reported experimental results are not consistent with each other. While Livi *et al.*[15] and Belošević-Čavor *et al.*[17] found that the measured HMF value at Ta site lies around ±8.5 T at room temperature, Akselrod *et al.*[16] reported that it is close to the $C15$ $HfFe_2$ HMF value of ±14.6 T at 300 K. Extrapolating the value of the HMF from Ref. 17 to 0 K (on basis of its reported temperature dependence), we obtain ±10.2 T. Our calculated value of −11.0 T, agrees well with this extrapolated value, which in turn indicates that the reported second component in the TDPAC spectrum originates from the $C14$ $HfFe_2$ structure. In $HfFe_2$ there is also a possibility of observing hyperfine interactions at the Fe sites by Mossbauer spectroscopy. Here, no supercell calculations are needed, as we compare the calculated HMF for the pure compound (without Ta) with the experimental data. The measured values[18,40] of 16.9 T at Fe $2a$ site and 18.8 T at Fe $6h$ site, are in excellent agreement with the calculated ones given in Table III, which is one additional confirmation of the quality of our calculations. Although there is lack of hyperfine interaction measurements for the $HfMn_2$ and $ZrMn_2$, we can emphasize one very interesting behavior of HMFs at Ta substituting on Hf(Zr) site. Namely, in the $ZrMn_2$, HMF is almost doubled, which is quite unexpected. On the other hand HMF in $HfMn_2$ shows the more usual behavior of decreasing with Ta inclusion, even though here it almost reaches zero.

In conclusion, we have calculated electric field gradients and hyperfine magnetic fields in a series of isostructural $C14$ Laves-phase compounds. We have found nonzero HMFs in $HfMn_2$ and $ZrMn_2$, which points out that these compounds possess strong magnetic ordering. We have offered a solution about the proper assignment of the measured hyperfine magnetic field value in the $C14$ $HfFe_2$ compound. The *ab initio* calculations with the supercell APW+lo method appear to be able to reproduce the experimental EFGs and HMFs to a high degree of precision.

---

[1] X. Q. Chen *et al.*, EPL **67**, 807 (2004).
[2] X. Q. Chen *et al.*, Phys. Rev. B **72**, 054440 (2005).
[3] X. Q. Chen, *et al.*, Phys. Rev. B **76**, 014424 (2007).
[4] I. Jacob and D. Shaltiel, J. Less-Common Met. **65**, 117 (1979).
[5] A. V. Skripov *et al.*, Phys. Rev. B **76**, 104305 (2007).
[6] D. Mukai *et al.*, J. Alloys Compd. **417**, 293 (1999).
[7] S. Hong and C. L. Fu, Phys. Rev. B **66**, 094109 (2002).
[8] A. Von Keitz and G. Sauthoff, Intermetallics **10**, 497 (2002).
[9] X. Q. Chen *et al.*, Phys. Rev. B **71**, 174101 (2005).
[10] X. Q. Chen *et al.*, J. Alloys Compd. **383**, 228 (2004).
[11] M. Rotter *et al.*, Phys. Rev. B **74**, 224109 (2006).
[12] S. Ishida *et al.*, J. Phys. Soc. Jpn. **54**, 3925 (1985).
[13] S. Asano and S. Ishida, J. Magn. Magn. Mater. **70**, 39 (1987).
[14] S. Asano, and S. Ishida J. Phys. F: Met. Phys. **18**, 501 (1988).
[15] F. P. Livi *et al.*, Phys. Status Solidi A **37**, 133 (1976).
[16] Z. Z. Akselrod *et al.*, Hyperfine Interact. **14**, 7 (1983).
[17] J. Belošević-Čavor *et al.*, J. Magn. Magn. Mater. **272-276**, 762 (2004).
[18] J. Belošević-Čavor *et al.*, Eur. Phys. J. B **50**, 425 (2006).
[19] I. I. Bulyk *et al.*, J. Alloys Compd. **367**, 283 (2004).
[20] J. Mestnik Filho *et al.*, J. Alloys Compd. **224**, 60 (1995).
[21] H. Anton and P. C. Schmidt, Intermetallics **5**, 449 (1997).
[22] V. K. Sinha and W. E. Wallace, J. Less-Common Met. **106**, 199 (1985).
[23] Ž. Blažina and R. Trojko, J. Less-Common Met. **133**, 277 (1987).
[24] H. Flandorfer *et al.*, Z. Metallkd. **88**, 529 (1997).
[25] L. D. Gulay and V. I. Zaremba, J. Alloys Compd. **347**, 184 (2002).
[26] R. P. Elliott, Trans. Am. Soc. Met. **53**, 321 (1961).
[27] J. H. Wernick and S. E. Haszko, J. Phys. Chem. Solids **18**, 207 (1961).
[28] V. N. Svechnikov and V. V. Petkov, *Metallofizika* (in Russion) (Academiya Nauk Ukrainskoi SSR, Institut Metallofiziki, 1976), Vol. 64, pp 24-29.
[29] J. L. Soubeyroux *et al.*, J. Alloys Compd. **231**, 760 (1995).
[30] D. K. Pandey *et al.*, Mater. Lett. **61**, 4747 (2007).
[31] K. Schwarz and P. Blaha, Comput. Mater. Sci. **28**, 259 (2003).
[32] A. R. Williams *et al.*, Phys. Rev. B **19**, 6094 (1979).
[33] J. P. Perdew *et al.*, Phys. Rev. Lett. **77**, 3865 (1996).
[34] F. D. Murnaghan, Proc. Natl. Acad. Sci. U.S.A. **30**, 244 (1944).
[35] P. Blaha *et al.*, Phys. Rev. Lett. **54**, 1192 (1985).
[36] J. Belošević-Čavor *et al.*, Comput. Mater. Sci. **41**, 164 (2007).
[37] J. Belošević-Čavor, *et al.*, Comput. Mater. Sci. **43**, 867 (2008).
[38] A. Kokalj, J. Mol. Graphics Modell. **17**, 176 (1999).
[39] S. Blugel *et al.*, Phys. Rev. B **35**, 3271 (1987).
[40] S. K. Xia *et al.*, J. Phys.: Condens. Matter **10**, 3457 (1998).